

—Supporting Information—

**Transparent Antismudge Coatings with Thermally Assisted
Healing Ability**

Fuchang Xu, Xiang Li, Dehui Weng, Yang Li and Junqi Sun*

State Key Laboratory of Supramolecular Structure and Materials, College of
Chemistry, Jilin University, Changchun 130012, PR China.

*E-mail: yanglichem@jlu.edu.cn

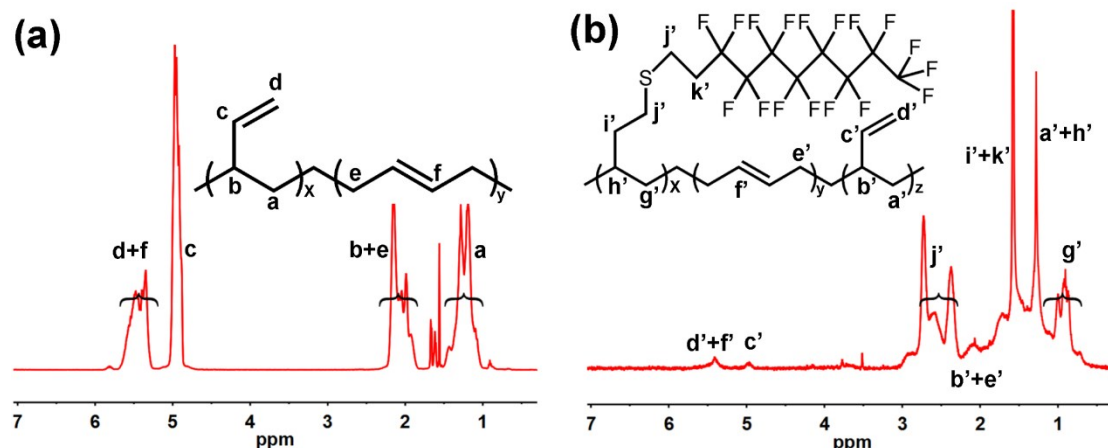


Fig. S1 ^1H -NMR (CDCl_3 , 500 MHz) spectra of (a) the PB and (b) the PB-g-PFDT.

The ^1H NMR spectrum of the PB in Fig. S1a are as follows: ^1H NMR (500MHz; CDCl_3 ; $(\text{CH}_3)_4\text{Si}$) mixture solution, δH 5.72-5.25 (4H, $\text{CH}_2=\text{C}-$, $-\text{CH}=\text{CH}-$), 4.96 (1H, m, $\text{C}=\text{CH}-\text{C}-$), 2.27-1.84 (3H, $-\text{C}=\text{C}-\text{CH}_2-$, $\text{C}=\text{CH}-\text{CH}(-\text{CH}_2-)_2$), 0.99-1.51 (m, 2H; $-\text{C}-\text{CH}_2-\text{C}-$)

The ^1H NMR spectrum of the PB-g-PFDT in Fig. S1b are as follows: ^1H NMR (500 MHz; CDCl_3 ; $(\text{CH}_3)_4\text{Si}$) mixture solution, δH 5.41 (3H, $\text{CH}_2=\text{C}$, $-\text{CH}=\text{CH}-$), 4.97 (1H, m, $\text{C}=\text{CH}-\text{C}-$), 2.25-3.05 (4H, t, $-\text{CH}_2-\text{S}-\text{CH}_2-$), 1.97-2.25 (3H, $-\text{C}=\text{CH}-\text{CH}(-\text{CH}_2-)_2$, $-\text{C}=\text{C}-\text{CH}_2-$), 1.57 (4H, t, $-\text{S}-\text{CH}_2-\text{CH}_2-$), 1.27 (3H, $-\text{C}-\text{CH}_2-\text{C}-\text{C}=\text{C}$, $-\text{CH}_2-\text{CH}(-\text{CH}_2-)_2$), 0.79-1.05 (2H, m, $-\text{CH}-\text{CH}_2-\text{CH}-$)

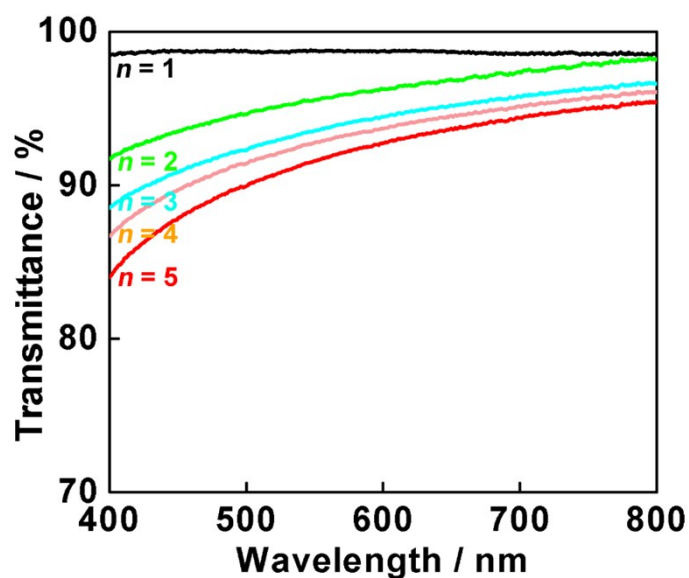


Fig. S2 Transmission spectra of the PB-g-PFDT_n coatings with *n* being 1-5.

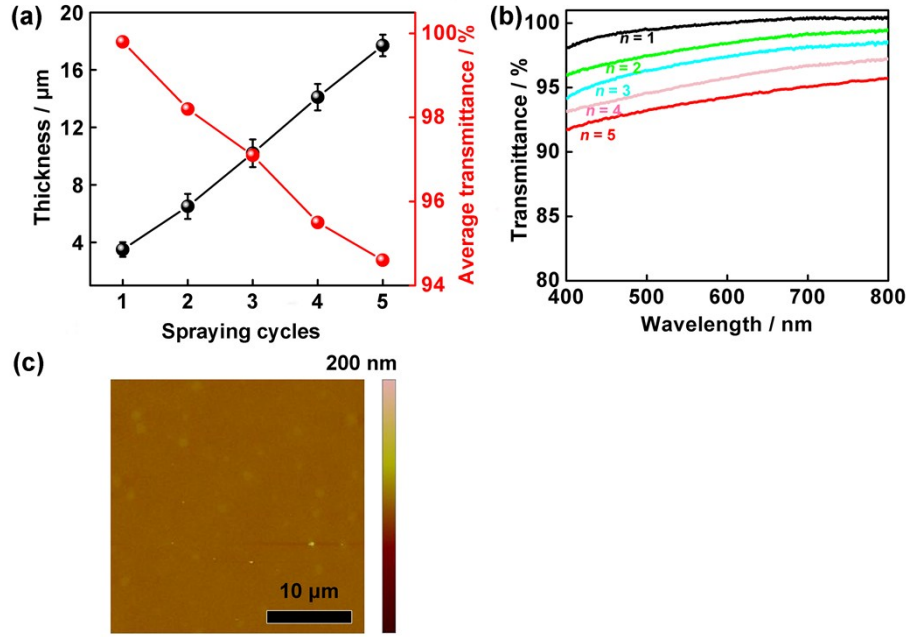


Fig. S3 (a) Thickness and average transmittance of the PB-g-PFDT_{*n*} coatings fabricated by spray coating as a function of spraying cycles. (b) Transmission spectra of the PB-g-PFDT_{*n*} coatings fabricated by spray coating as a function of spraying cycles. (c) AFM image of the PB-g-PFDT₅ coating fabricated by spray coating.

The THF/HFIP binary solution of PB-g-PFDT (30 mg mL⁻¹) was sprayed onto the glass substrates (2 × 3 cm²) by using a spray gun (Infinity CRplus, Harder & Steenbeck) with a 0.4-mm nozzle, followed by drying at room temperature for 10 min. The spray volume was 0.083 mL cm⁻², the operating pressure of the spray gun was 0.2 MPa and the distance between the nozzle and the substrate was 7 cm. The spraying and drying processes were repeated until the desired cycles were reached. Finally, the PB-g-PFDT_{*n*} coatings were annealed at 100°C for 2 h. As shown in Fig. S3a, the thickness of the PB-g-PFDT_{*n*} coating linearly increases with the increase in spray coating cycle, with an average thickness increase of ~3.5 μm per cycle. The PB-g-PFDT₅ coating has a thickness and an average transmittance of $17.7 \pm 0.8 \mu\text{m}$ and 94.6% (Fig. S3a and b), which are similar to that of the PB-g-PFDT₃ coating fabricated by bar coating. In addition, Fig. S3c shows that the RMS roughness of the resulting PB-g-PFDT₅ coating is 4.9 nm, which is similar to that of the PB-g-PFDT₃ coating fabricated by bar coating. All these results suggest that spray coating can be employed to fabricate the PB-g-PFDT_{*n*} coatings with controllable thicknesses.

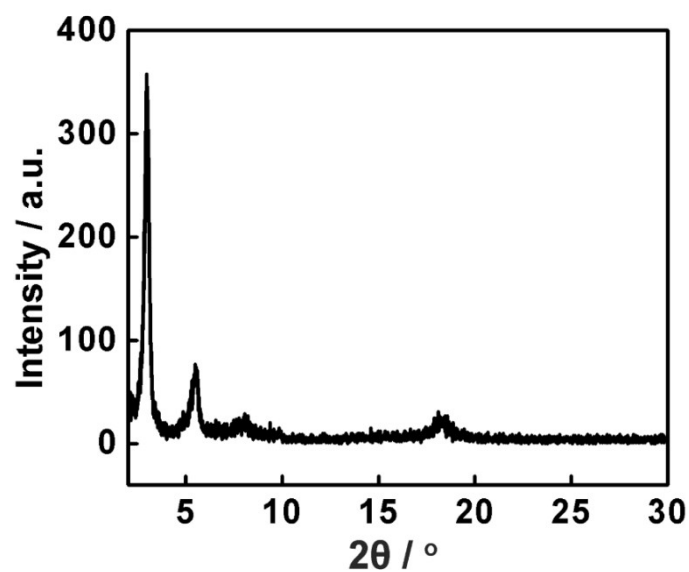


Fig. S4 XRD spectrum of the PB-g-PFDT₃ coating.

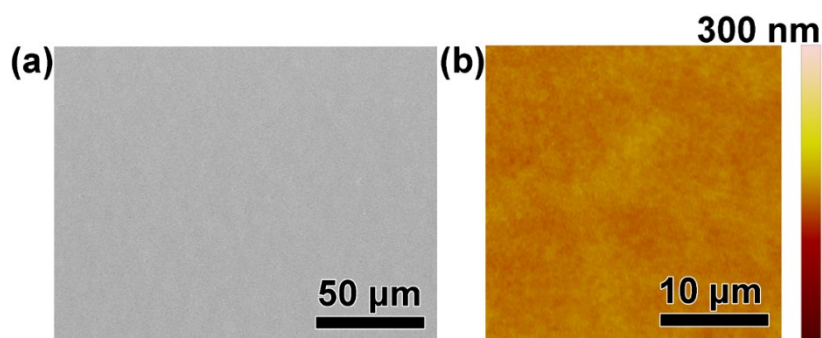


Fig. S5 (a) Top-view SEM and (b) AFM images of the surface of the PB-g-PFDT₃ coatings.

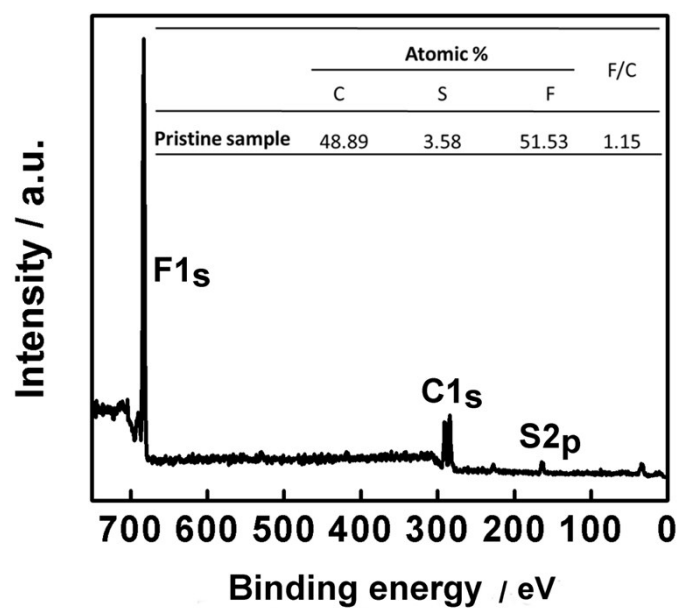


Fig. S6 XPS spectrum of the surface of the PB-g-PFDT₃ coating.

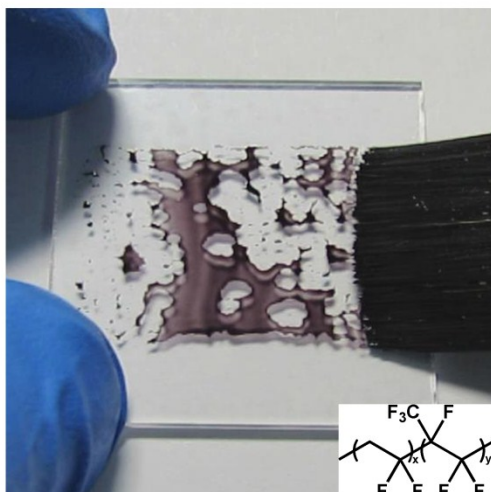


Fig. S7 Antismudge performance of the PVDF-co-HFP₃-coated glass. Inset: Molecular structure of the PVDF-co-HFP.

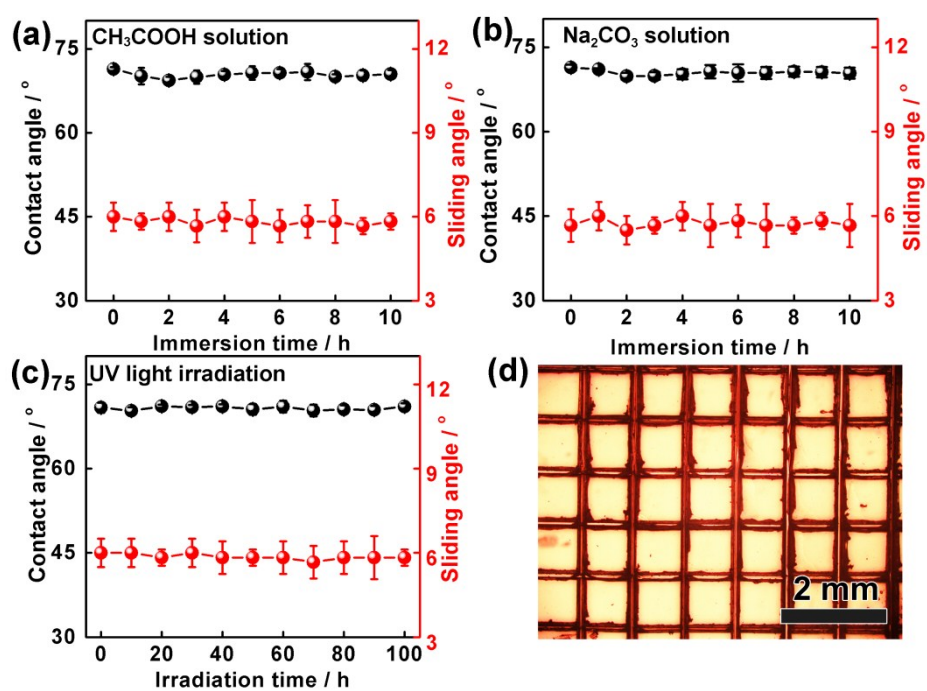


Fig. S8 CAs and SAs of decane droplets on the PB-g-PFDT₃ coatings after immersion in (a) CH₃COOH (1 wt%, pH = 2.75) and (b) Na₂CO₃ (1 wt%, pH=11.65) solutions or (c) irradiation under UV light for different time. (d) Microscope image of the PB-g-PFDT₃ coating after tape test.

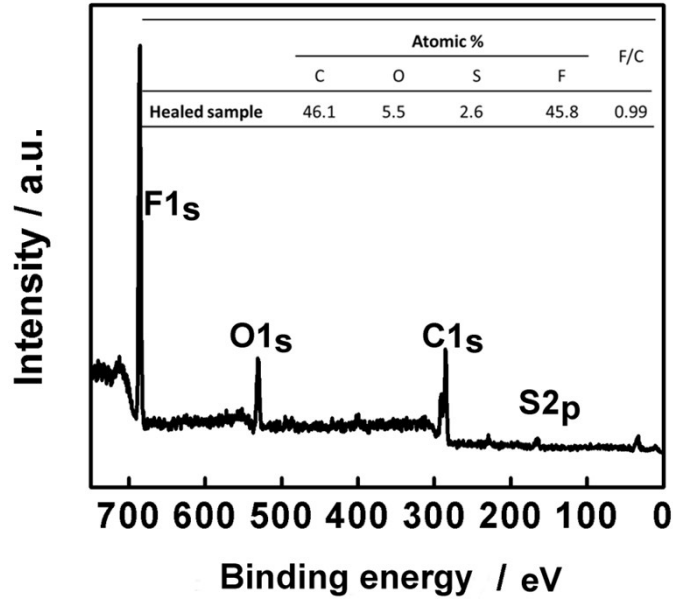


Fig. S9 XPS spectrum of the healed PB-g-PFDT₃ coating.

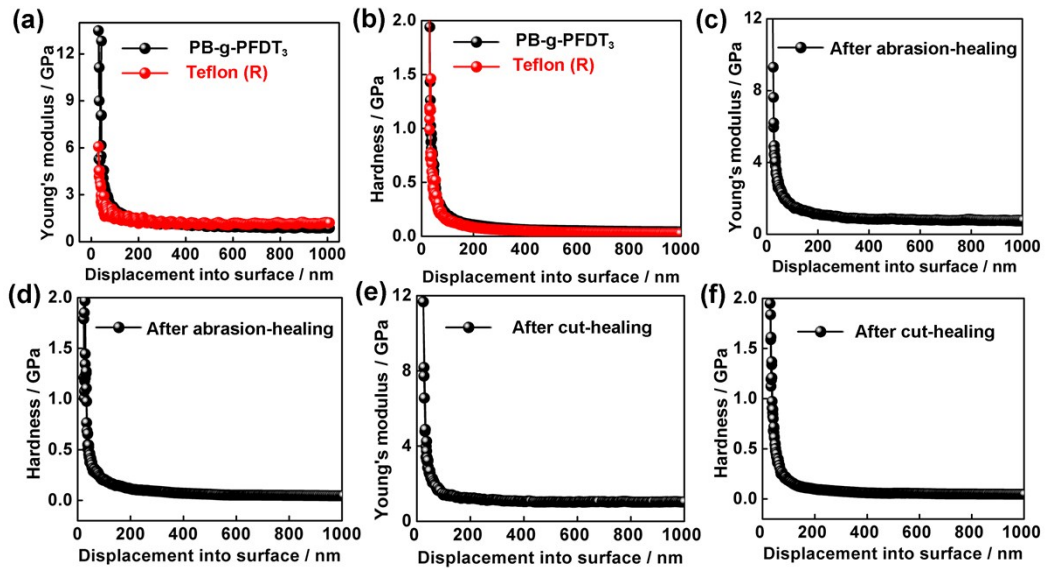


Fig. S10 Young's moduli (E) and hardness (H) of (a) the PB-g-PFDT₃ coating and (b) a commercial Teflon (R). (c, d) E and H of the scratched PB-g-PFDT₃ coating after healing. (e, f) E and H of the healed area on the cut PB-g-PFDT₃ coating after healing.

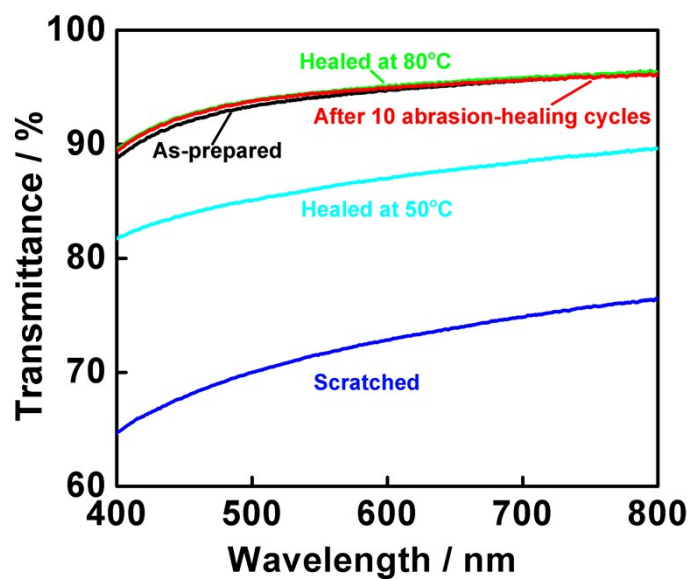


Fig. S11 Transmission spectra of the as-prepared PB-g-PFDT₃ coating, the scratched PB-g-PFDT₃ coating, the scratched PB-g-PFDT₃ coating after heating at 50°C and 80°C, and the PB-g-PFDT₃ coating after 10 abrasion-healing cycles.

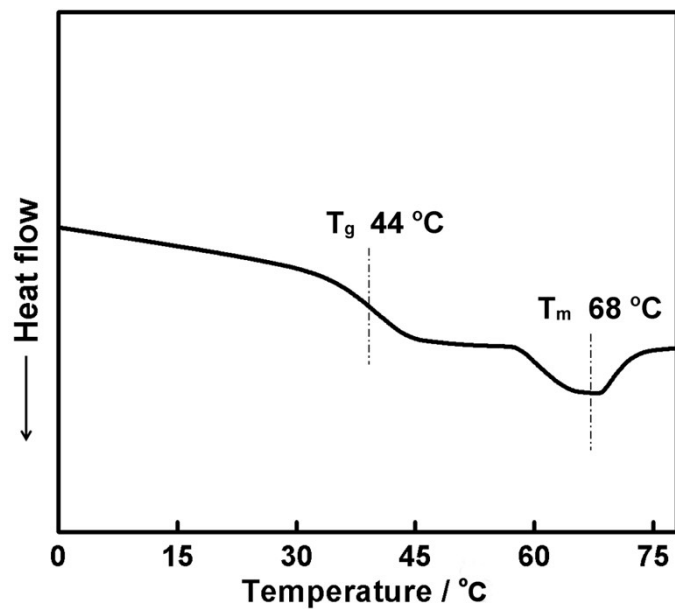


Fig. S12 DSC spectrum of the PB-g-PFDT.

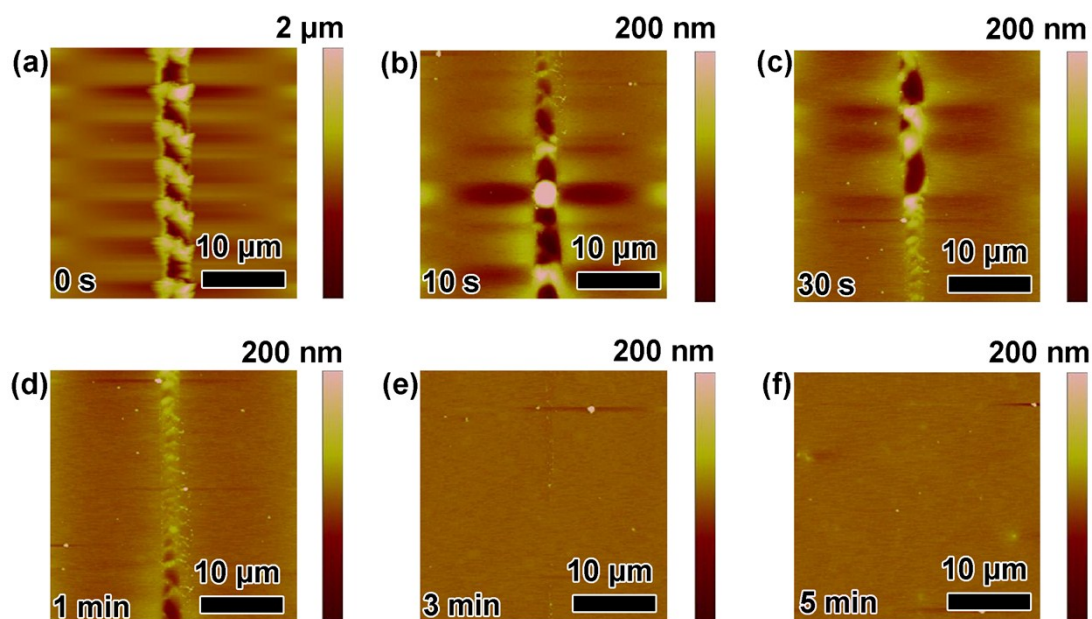


Fig. S13 AFM images of a scratch on the scratched PB-g-PFDT₃ coating after heating at 80°C for different times.

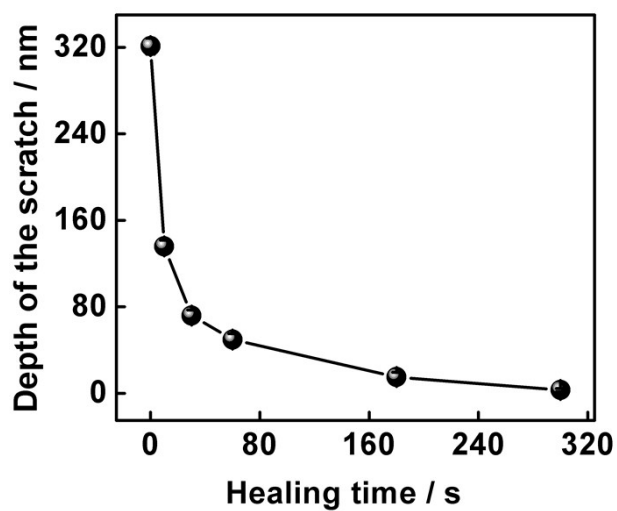


Fig. S14 Depth of the scratch in Fig. S13a after heating at 80°C for different times.

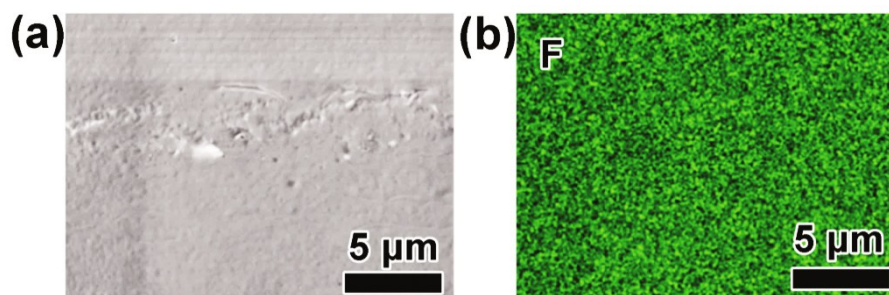


Fig. S15 (a) SEM image and (b) SEM-EDX map for F of healed area on the PB-g-PFDT₃ coating.

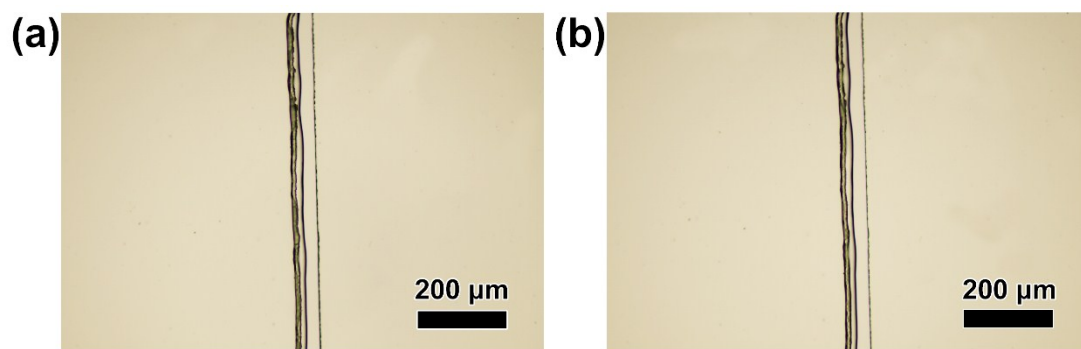


Fig. S16 Microscope images of the cut on the PVDF-co-HFP₃ coating before (a) and after (b) heating for 2 h at 140 °C.

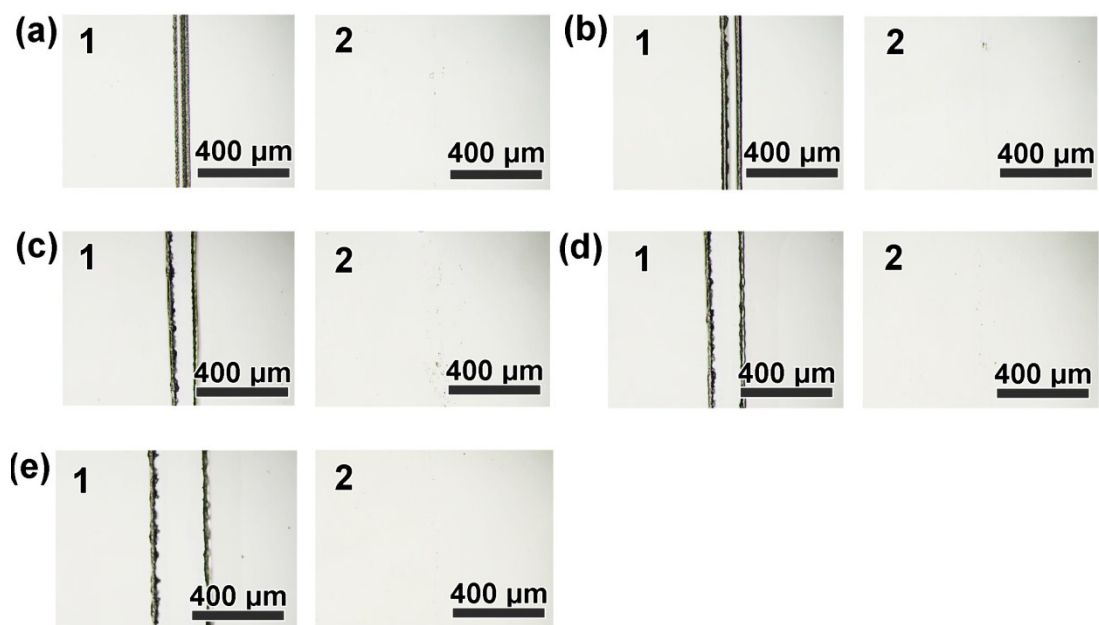


Fig. S17 (a-e) Microscope images of the cuts on the PB-g-PFDT _{n} coatings with n being 1-5 before (1) and after (2) heating.